SUPPLEMENTARY DATA 1: Supplementary data to Genome-Wide Association

Genomic Samples Characteristics. All 24 genomics data were archived into the Gene Expression Omnibus (GEO) repository supporting a compliance with Minimum Information About a Microarray Experiment (MIAME). The verified pathological reports of these patients indicated tumor grades G1 to G3 of type IIIA minimum stage grouping in accordance with the American Joint Committee on Cancer (AJCC) staging. All 24 patients were males with ages ranging from 26 years to 86 years. There were some matched tissues from the same patient for a total of 10 hepatocellular carcinomas, 6 cirrhosis, and 8 normal livers (i.e. non-carcinoma and non-cirrhosis) with RNA integrity numbers ranging from 8.1 to 9.6. The RNA quality/purity determined by UV absorbance (A_{260}/A_{280} ratio) ranged from 2.07 to 2.20.

Table 1S: Patients and samples descriptions.

Sample ID	Facility ID	Pathology	Gender	Age	Paired	RIN
CR561042	44681	CL	male	43	A	8.9
CR561021	44682	HCC	male	43	A	9.3
CR562704	44677	NL	male	86	B	9
CR562705	44679	HCC	male	86	B	9.5
CR561125	44675	CL	male	71	C	9.2
CR560983	44676	HCC	male	71	C	9.3
CR562996	46243	HCC	male	71	D	9.50
CR562969	44678	NL	male	71	D	8.1
CR559270	46236	HCC	male	26	E	9.60
CR561701	46237	FL	male	26	E	8.90
CR562998	46238	HCC	male	56	F	9.10
CR563039	46239	FL	male	56	F	9.40
CR561944	44680	NL	male	68	G	8.4
CR562008	46240	CL	male	77	H	9.30
CR562293	46241	CL	male	50	I	9.20
CR562477	46242	CL	male	60	J	9.40
CR561038	49156	HCC	male	73	K	8.80
CR561037	49154	NL	male	73	K	8.90
CR561794	49157	NL	male	66	L	9.20
CR561793	49169	HCC	male	66	L	7.90
CR562478	49158	HCC	male	60	M	8.90
CR562477	49159	CL	male	60	M	9.00
CR561272	49155	NL	male	81	N	9.20
CR562589	49160	HCC	male	79	O	9.00

Table 1: Patients and samples descriptions in the study: Hepatocellular carcinoma (HCC); Cirrhosis of liver (CL); Fatty changes of liver (FL); Normal liver (NL); RNA integrity number (RIN); Identification (ID). Note that the fatty changes of liver were grouped with normal liver.

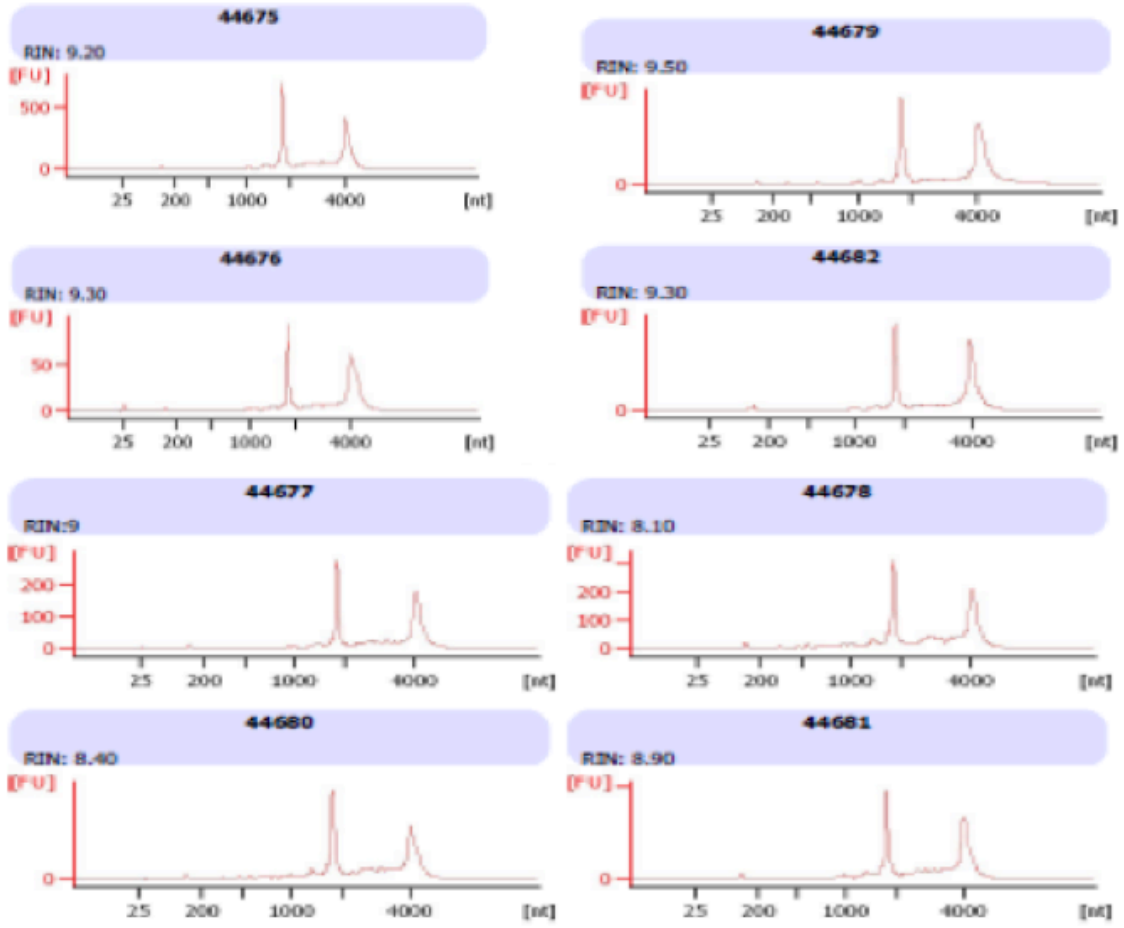

Figure 1S: Electropherograms of samples in project ID number 4518 where each five-digit label represents the facility ID of the sample. A plot of fluorescence units (FU) versus amount of nucleotides (nt). The Bioanalyzer electropherogram of total RNA shows two distinct ribosomal peaks corresponding to either 18S (2125 nt) or 28S (4375 nt) for eukaryotic RNA and a relatively flat baseline between the 5S (156 nt) and 18S ribosomal peaks. Microfluidic analysis was performed using the Agilent® 2100 Bioanalyzer with an RNA LabChip Kit to calculate the RNA Integrity Number (RIN) used to evaluate RNA integrity. The integrity of the RNA sample, or the proportion that is full length, is an important component of RNA quality. Reverse transcribing partially degraded mRNA may generate cDNA that lacks parts of the coding region.

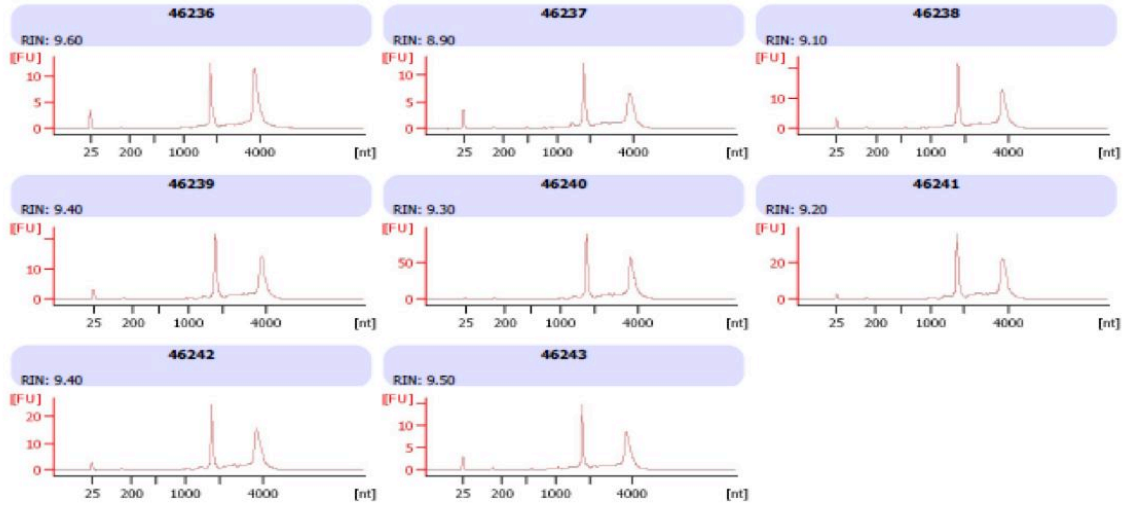

Figure 2S: Electropherograms of samples in project ID number 4610 where each five-digit label represents the facility ID of the sample. A plot of fluorescence units (FU) versus amount of nucleotides (nt). The Bioanalyzer electropherogram of total RNA shows two distinct ribosomal peaks corresponding to either 18S (2125 nt) or 28S (4375 nt) for eukaryotic RNA and a relatively flat baseline between the 5S (156 nt) and 18S ribosomal peaks. Microfluidic analysis was performed using the Agilent® 2100 Bioanalyzer with an RNA LabChip Kit to calculate the RNA Integrity Number (RIN) used to evaluate RNA integrity. The integrity of the RNA sample, or the proportion that is full length, is an important component of RNA quality. Reverse transcribing partially degraded mRNA may generate cDNA that lacks parts of the coding region.

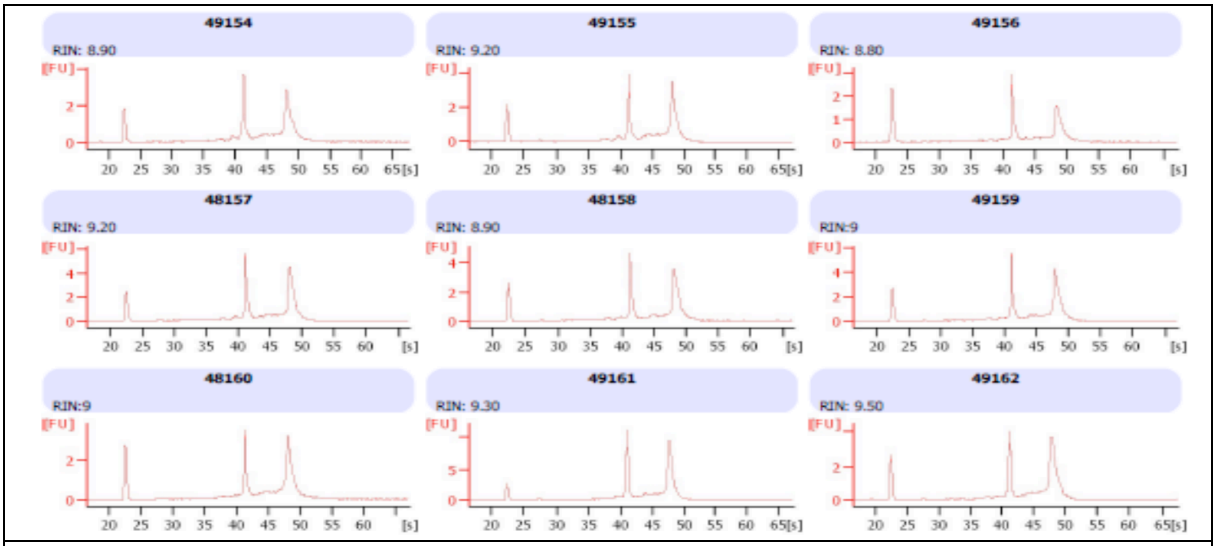

Figure 3S: Electropherograms of samples in project ID number 4807 where each five-digit label represents the facility ID of the sample. A plot of fluorescence units (FU) versus amount of nucleotides (nt). The Bioanalyzer electropherogram of total RNA shows two distinct ribosomal peaks corresponding to either 18S (2125 nt) or 28S (4375 nt) for eukaryotic RNA and a relatively flat baseline between the 5S (156 nt) and 18S ribosomal peaks. Microfluidic analysis was performed using the Agilent® 2100 Bioanalyzer with an RNA LabChip Kit to calculate the RNA Integrity Number (RIN) used to evaluate RNA integrity. The integrity of the RNA sample, or the proportion that is full length, is an important component of RNA quality. Reverse transcribing partially degraded mRNA may generate cDNA that lacks parts of the coding region.

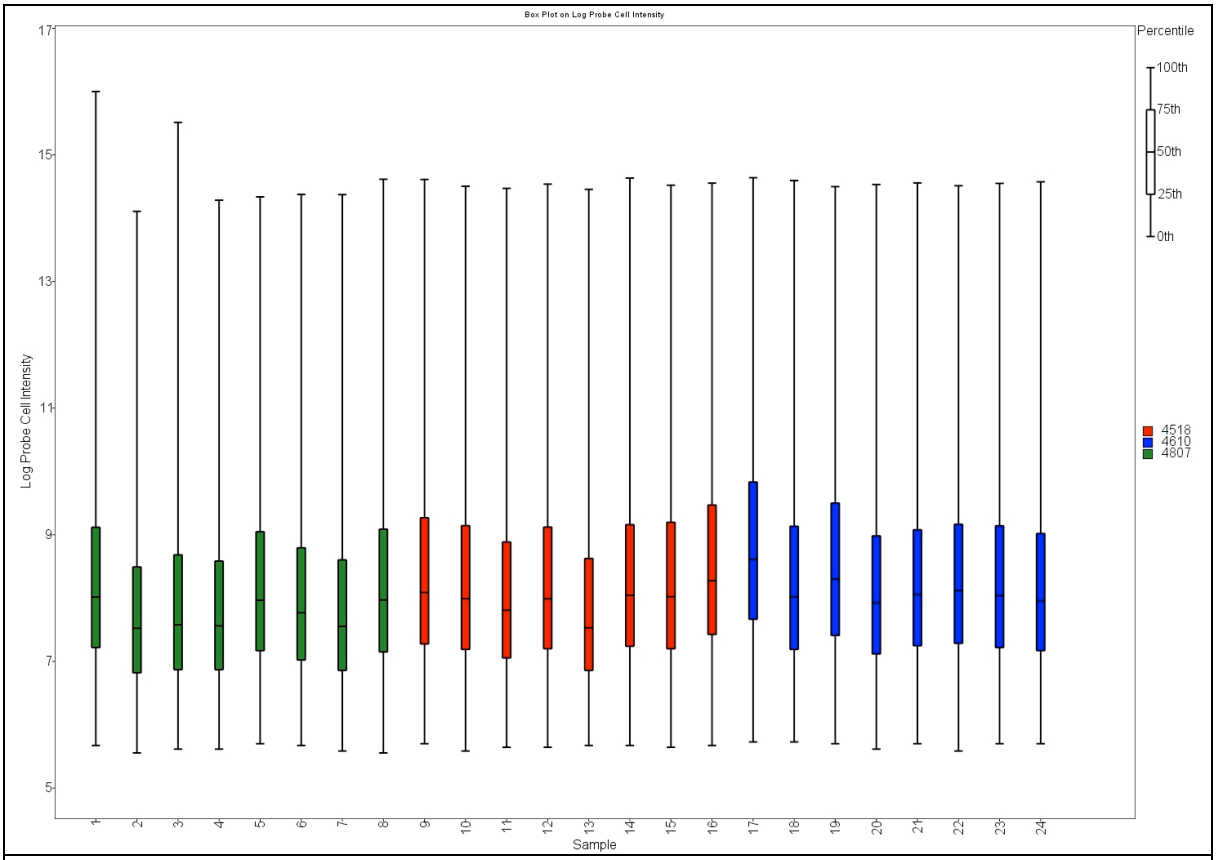

Figure 4S: Hybridization Quality Control Array Data. Signal Box Plot displaying the distribution of the data at level of summarized probe sets as analyzed using Robust Multichip Analysis (RMA) normalization. Note the extremely similar plots due to quintile normalization of data.

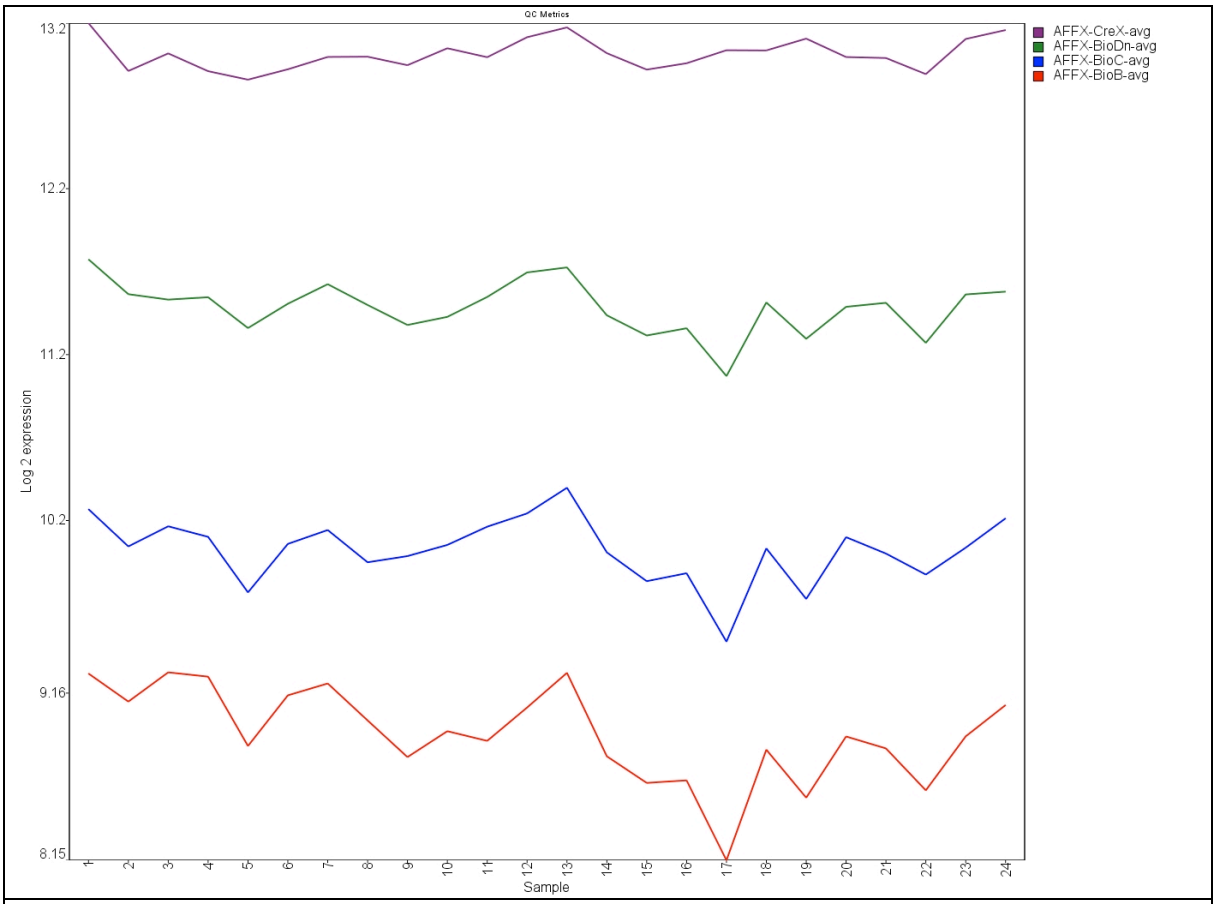

Figure 5S: Hybridization Quality Control Array Data. Hybridization Control spikes shown in line graphs for all 16 arrays. Note that the hybridization controls are in the expected order according to their concentrations (synthetic: BioB 1.5 pM; BioC 5 pM; BioD 25 pM; Cre 100 pM).

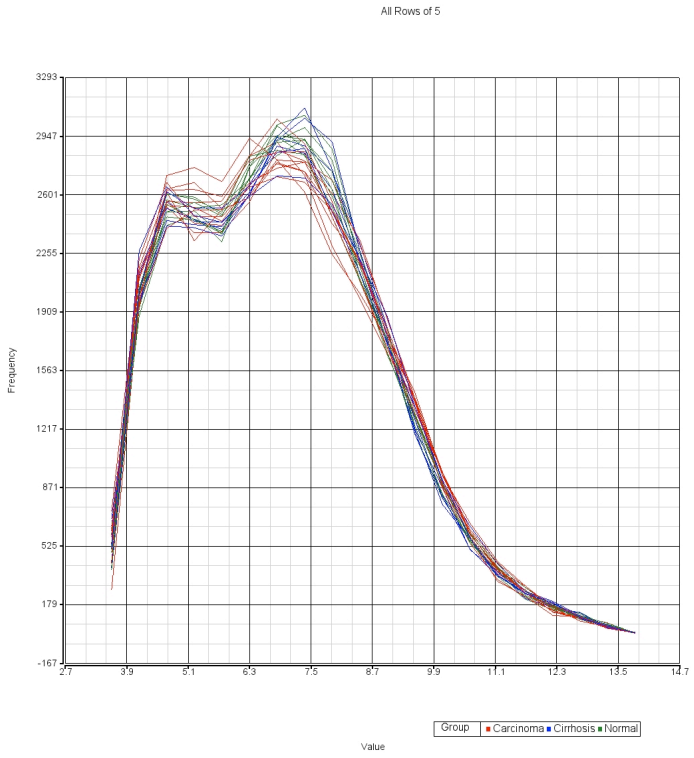

Figure 6S: Histogram of Robust Multichip Analysis (RMA) derived probe set log_2 intensities. Note minor outlier in project ID data. Assessing hybridization quality using sample histogram.

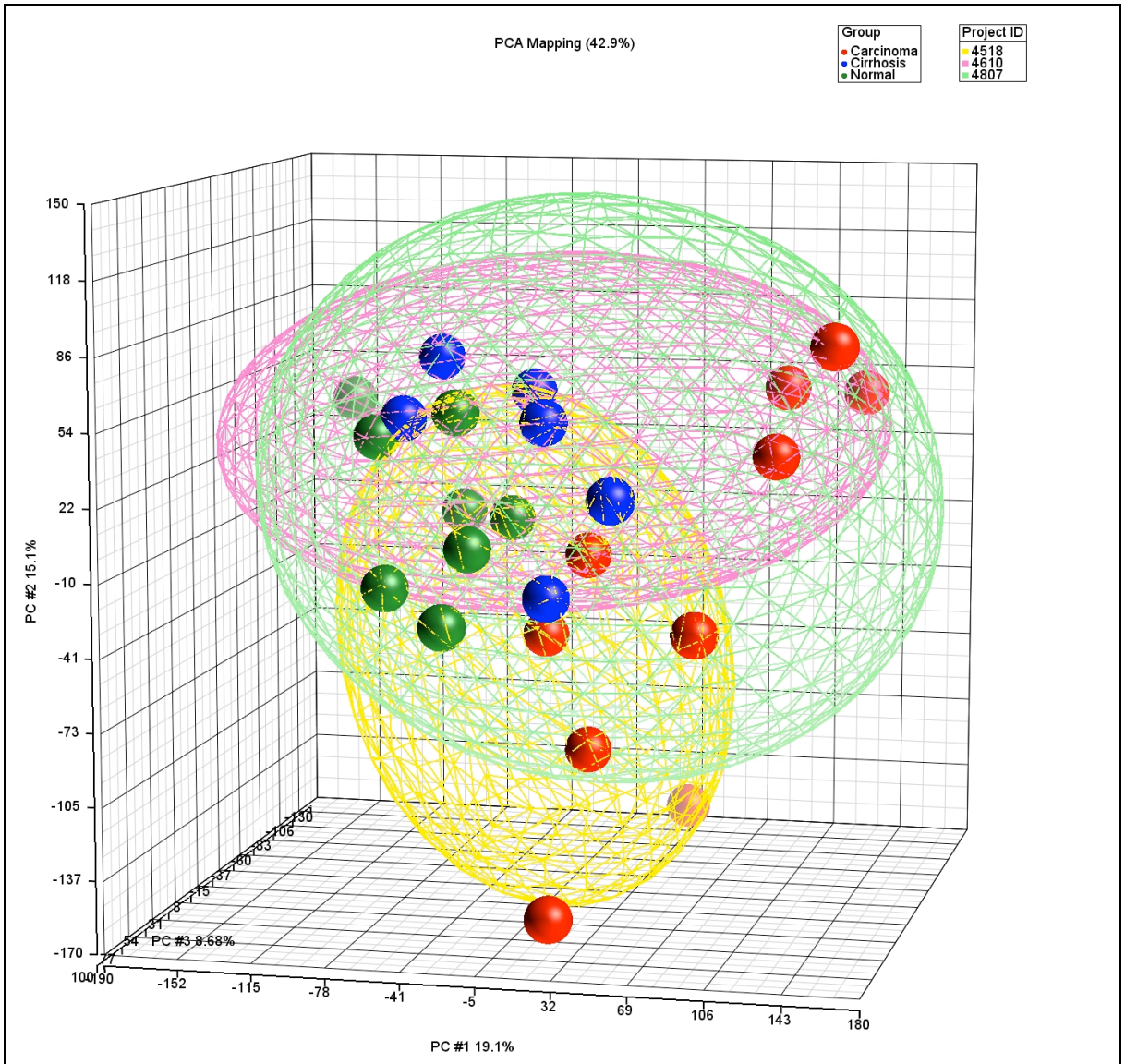

Figure 7S: Assessing Hybridization Quality Using PCA. Principal Components Analysis (PCA) in three-dimensional plot of all hybridizations showing individual samples from patients and the ellipsoids drawn at two standard deviations from the project ID centric (i.e. three separate experiments of different patients).

SUPPLEMENTARY DATA 2: MR SPECTRA SAMPLES – <u>Supplementary data to high-resolution magnetic resonance spectroscopy experiments for perchloric acid extracts of tissues</u>.

MR spectroscopy was performed at 400MHz on a Broker Advance III™ wide-bore spectrometer using the Topspin Broker software. Each lyophilized tissue extract was dissolved in 0.45 mL of D_2O, the pH adjusted to 7.0 and the solution introduced in a 5 mm NMR tube. An external standard made of a sealed capillary containing a solution of trimethylsilylpropionic acid (TSP) in D_2O was introduced in the NMR tube. The TSP capillary was used as chemical shift reference and quantitation standard. Fully relaxed proton spectra were acquired with a 5 mm BBO probe. Standard acquisition conditions were as follows: pulse width (PW) 45°, repetition time (TR) 8 s, water saturation during the relaxation delay, sweep width (SW) 6.7 kHz, data point (TD) 64 k, 4 dummy scans and 64 scans. Following the ^{1}H NMR 0.150 µL of 50 mM EDTA was added to the sample, the pH adjusted to 8.0 and a sealed calibrated capillary of methylene diphosphonate (MDP) was introduced in the NMR tube. Phosphorus spectra were acquired with the inversegate pulse program and the following conditions: SW 13 kHz, TD 64 k, AQ 2.5 s, D1 1.5 s, PW 45°, TR 4 s, 128 dummy scans, 2000 scans. Under these acquisition conditions the phosphorus signals are fully relaxed except for the inorganic phosphate (Pi).

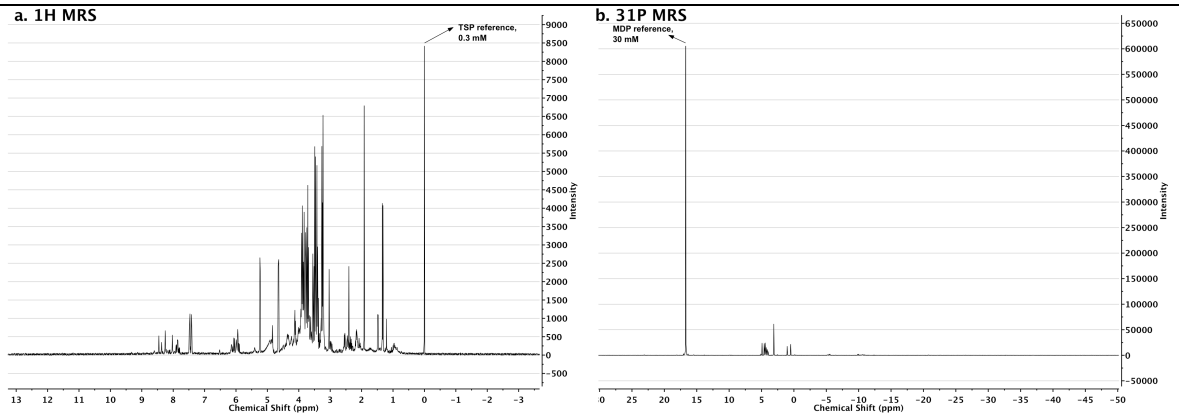

Figure 8S: Representative high-resolution MRS spectra from **human liver tissues** after perchloric acid extraction. [**a**] ^{1}H MRS spectrum identifying reference against trimethylsilyl propanoic acid (TSP) and the **corresponding** [**b**] ^{31}P MRS spectrum identifying referenced against methylene diphosphonate (MDP).

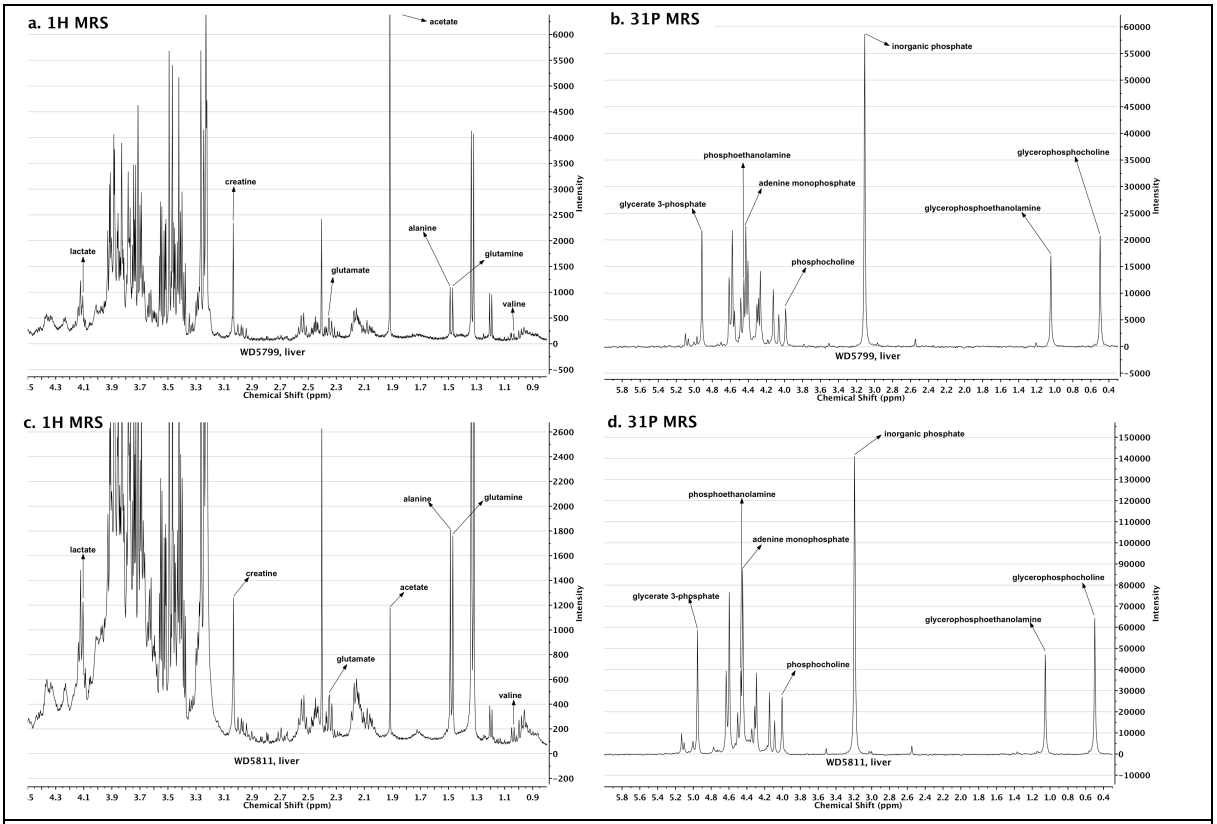

Figure 9S: Representative high-resolution MRS spectra from **normal human liver tissues** after perchloric acid extraction. [**a & c**] ^{1}H MRS spectrum identifying valine (CH_3 at 1.03 ppm), acetate (CH_3 at 1.93 ppm), succinate (CH_2 at 2.4 ppm), creative (CH_3 at 3.03 ppm) alanine (CH_3 at 1.47 ppm), glutamate (CH_2 at 2.35 ppm), glutamine (CH_2 at 2.145 ppm), and lactate (CH at 4.1) and the **corresponding** [**b & d**] ^{31}P MRS spectrum identifying glucose-6-phosphate (Glu6P), glycerate-3-phosphate (Gly3P), phosphoethanolamine (PE), phosphocholine (PC); (d) glycerophosphoethanolamine (GPE), glycerophosphocholine (GPC), adenine monophosphate (AMP), and inorganic phosphate (Pi), **respectively**. All metabolites are referenced against TSP or MDP.

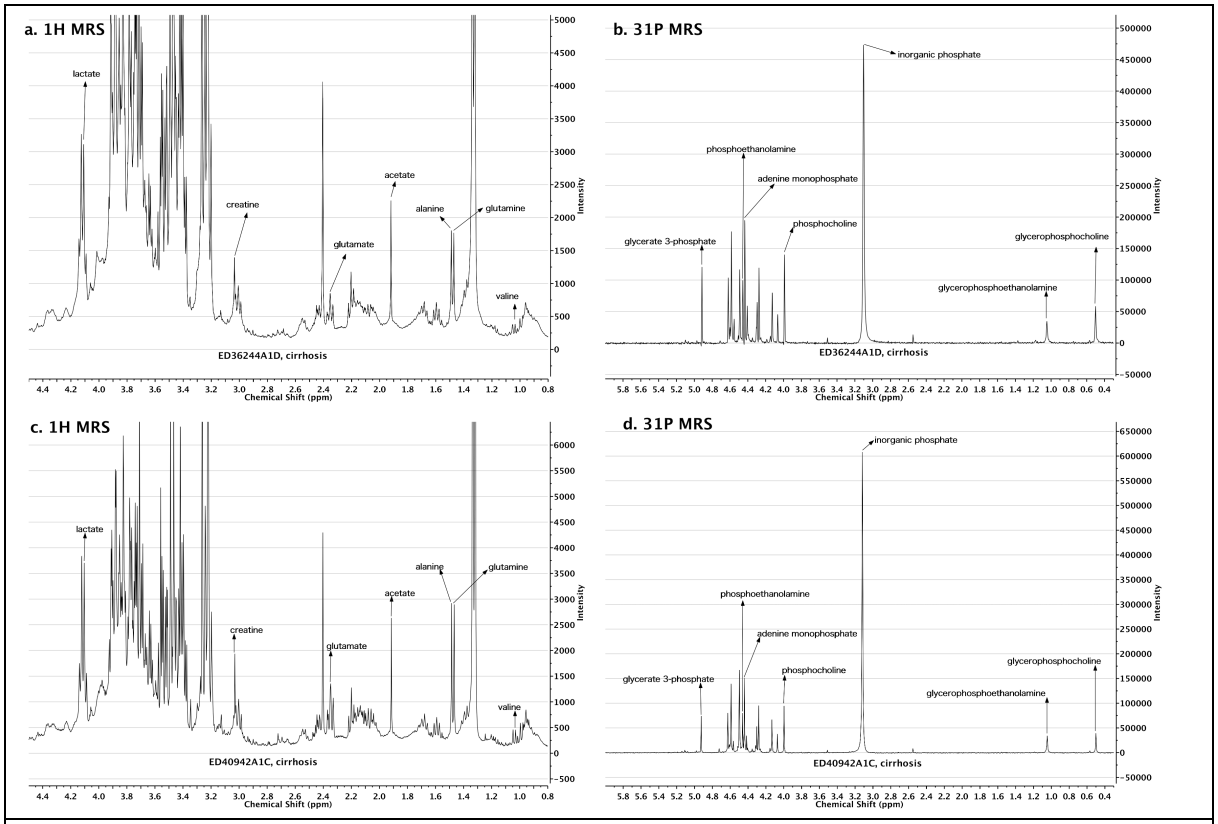

Figure 10S: Representative high-resolution MRS spectra from **human liver cirrhosis tissues** after perchloric acid extraction. [**a & c**] ^{1}H MRS spectrum identifying valine (CH_3 at 1.03 ppm), acetate (CH_3 at 1.93 ppm), succinate (CH_2 at 2.4 ppm), creative (CH_3 at 3.03 ppm) alanine (CH_3 at 1.47 ppm), glutamate (CH_2 at 2.35 ppm), glutamine (CH_2 at 2.145 ppm), and lactate (CH at 4.1) and the **corresponding** [**b & d**] ^{31}P MRS spectrum identifying glucose-6-phosphate (Glu6P), glycerate-3-phosphate (Gly3P), phosphoethanolamine (PE), phosphocholine (PC); (d) glycerophosphoethanolamine (GPE), glycerophosphocholine (GPC), adenine monophosphate (AMP), and inorganic phosphate (Pi), **respectively**. All metabolites are referenced against TSP or MDP.

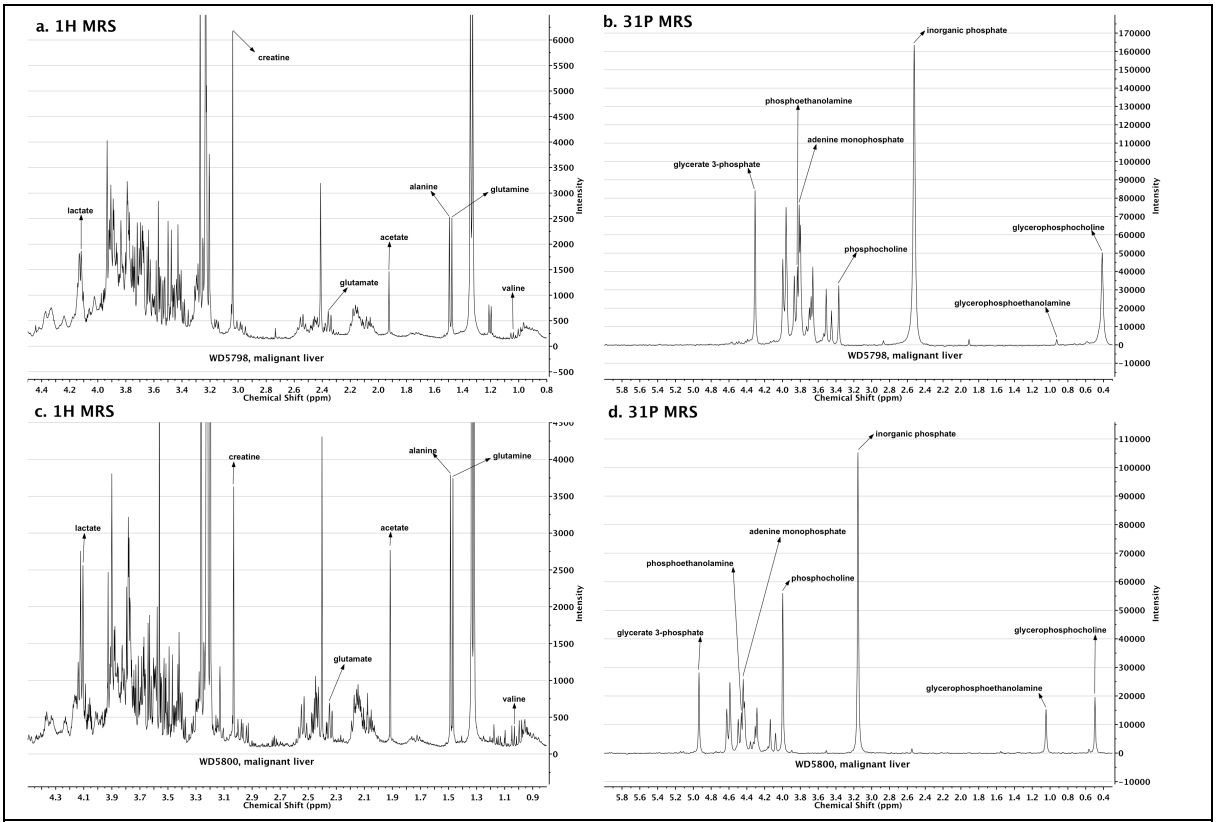

Figure 11S: Representative high-resolution MRS spectra from **human malignant liver (HCC) tissues** after perchloric acid extraction. [**a & c**] ^{1}H MRS spectrum identifying valise (CH_3 at 1.03 ppm), acetate (CH_3 at 1.93 ppm), succinate (CH_2 at 2.4 ppm), creative (CH_3 at 3.03 ppm) alanine (CH_3 at 1.47 ppm), glutamate (CH_2 at 2.35 ppm), glutamine (CH_2 at 2.145 ppm), and lactate (CH at 4.1) and the **corresponding** [**b & d**] ^{31}P MRS spectrum identifying glucose-6-phosphate (Glu6P), glycerate-3-phosphate (Gly3P), phosphoethanolamine (PE), phosphocholine (PC); (d) glycerophosphoethanolamine (GPE), glycerophosphocholine (GPC), adenine monophosphate (AMP), and inorganic phosphate (Pi), **respectively**. All metabolites are referenced against TSP or MDP.

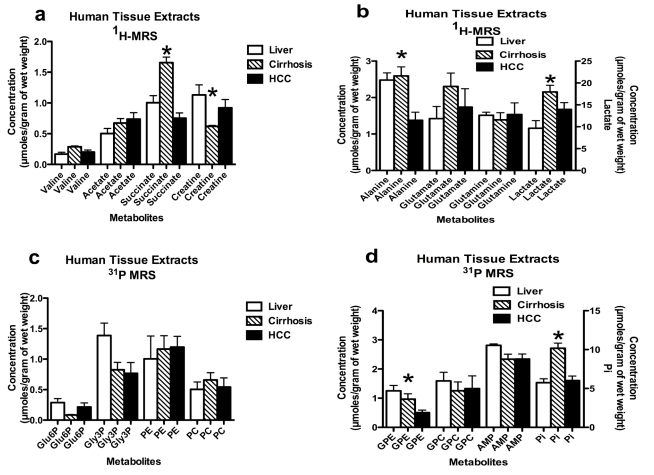

Figure 12S: Summary of the detectable metabolite concentrations from human liver tissues (i.e. HCC, cirrhosis, non-tumor) after perchloric acid extraction. (**a**) valine, acetate, succinate, and creatine; (**b**) alanine, glutamate, glutamine, and lactate; (**c**) glucose-6-phosphate (Glu6P), glycerate-3-phosphate (Gly3P), phosphoethanolamine (PE), phosphocholine (PC); (**d**) glycerophosphoethanolamine (GPE), glycerophosphocholine (GPC), adenine monophosphate (AMP), and inorganic phosphate (Pi). All metabolites are referenced against MDP or TSP. All bar graphs are displayed as mean±SEM, and the p-values were evaluated by oneway-ANOVA (^{ns}p-value>0.05, *p-value≤0.05, **p-value≤0.01).

SUPPLEMENTARY DATA 3: LC-MS/MS CHROMATOGRAMS – <u>Supplementary data to liquid-chromatography mass spectrometry experiments.</u>

Morris hepatoma McA-RH7777 cells were cultured in 75 cm^2 flasks for 48-72 h to 70% confluence in formulated Dulbecco's Modified Eagle's Medium (DMEM) supplemented with fetal bovine serum to a final concentration of 10% (v/v). The cells and culture media were obtained from American Type Culture Collection (ATCC), Manassas, VA. DMEM contained 4 mM L-glutamine, 24.98 mM glucose, 1 mM pyruvate and 17.86 mM sodium bicarbonate. A 24.98 mM [U-$^{13}C_6$]glucose (Sigma Chemical Co., St. Louis, MO) stock solution was prepared in glucose free DMEM. Cells were split and cultured with labeled or unlabeled glucose for 6 hours in an incubator at 37°C and 5% carbon dioxide in air. In a separate experiment, 2.48 mM [U-$^{13}C_5$,$^{15}N_2$]glutamine (Sigma Chemical Co., St. Louis, MO) stock solution was prepared in glucose and glutamine free DMEM. Similarly in the separate experiment, cells split and cultured with labeled or unlabeled glutamine and for 6 hours in an incubator at 37°C and 5% carbon dioxide in air. The cells were harvested with 25% Trypsin-0.53 mM EDTA, counted with a hemacytometer, and 13.3×10^6 cells were analyzed in triplicate. Cell suspension was transferred to centrifuge tubes and spun at 125 ×*g* for 10 minutes. Cell pellets were resuspended in 500 uL of 10% trichloroacetic acid for CoA-species extraction or 500 μL of 80% methanol for organic acids extraction. The CoA-species were stabilized with 5% sulfo-salicylic acid (SSA). The organic acids were derivatived with methoxylamine and N-tert-butyldimethylsilyl-N-methyltrifluoro acetamide (MTBSTFA) or derivatized with MTBSTFA alone. The methoxylamine derivatization was performed in pyridine to specifically detect the α-ketoglutarate metabolite. Intermediate metabolites of glycolysis and the TCA cycle were analyzed by the multiple reaction monitoring methodology of LC-MS as previously described for CoA species (1) and LC-MS/MS method was used for organic acids (2) by using an API 4000 Triple quadrapole mass spectrometer (Applied Biosystems, Foster City, CA) in the positive electrospray ionization (ESI) mode. A matrix-based isotopomer analysis (3,4) was performed for quantification of [U-$^{13}C_6$]glucose isotopic enrichment into the TCA cycle metabolites using custom script written in Matlab (The MathWorks, Inc., Natick, MA, USA).

References:

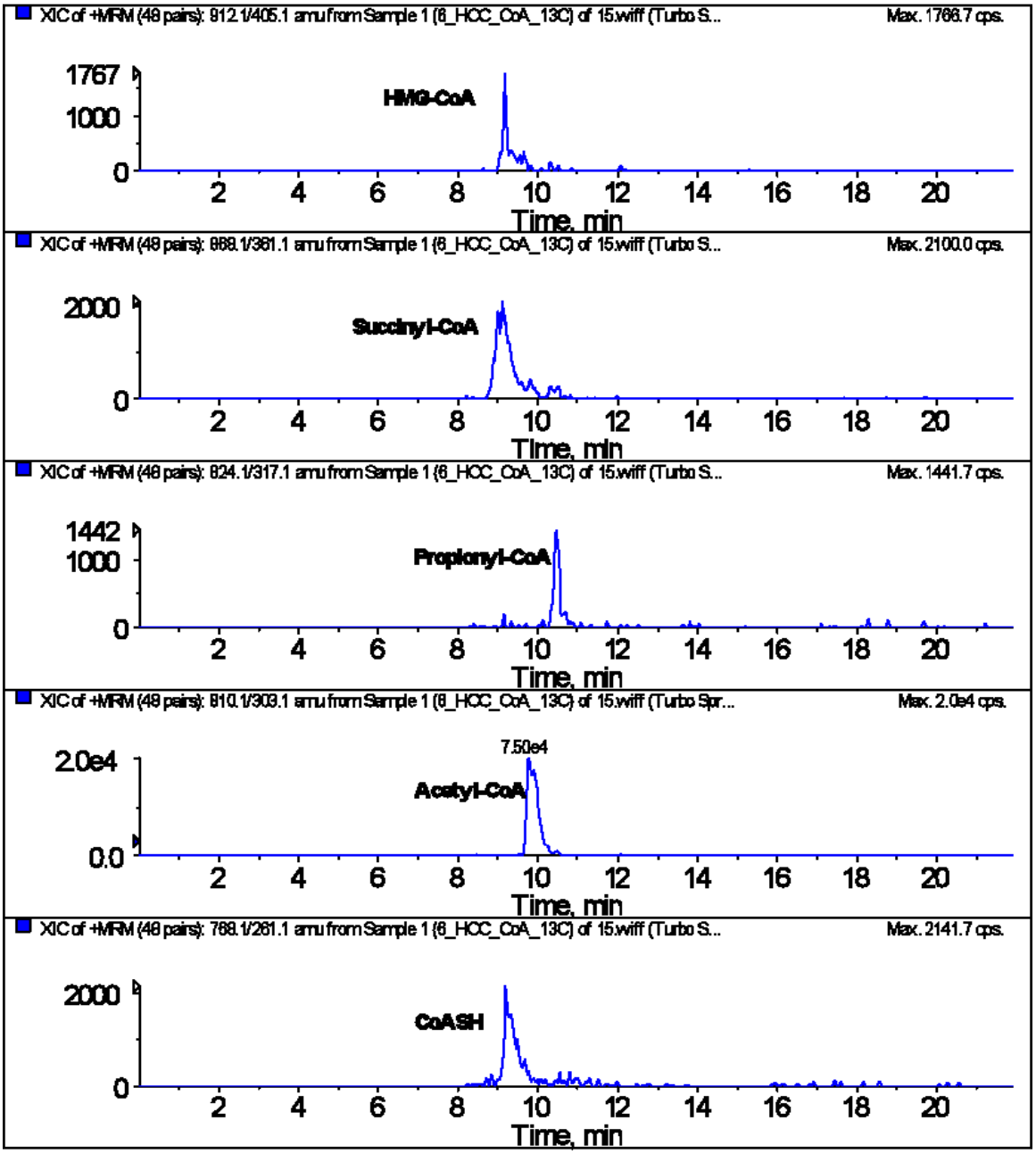

Figure 13S: LC-MS/MS Chromatograms of ^{13}C-labeled CoA-species from HCC cells. Plotted as signal intensity (cps, counts per second) versus retention time (min, minute).

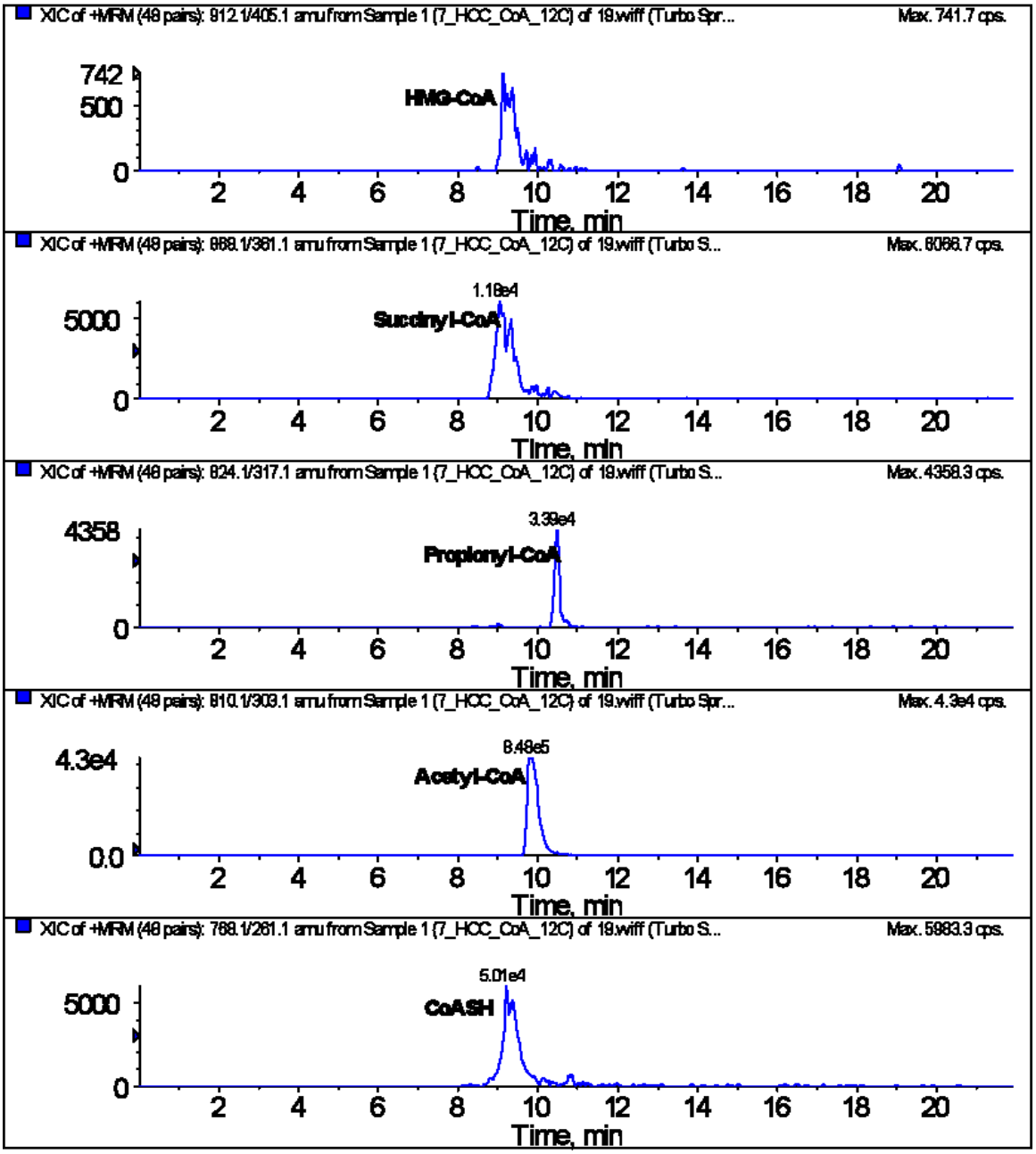

Figure 14S: LC-MS/MS Chromatograms of unlabeled CoA-species from HCC cells. Plotted as signal intensity (cps, counts per second) versus retention time (min, minute).

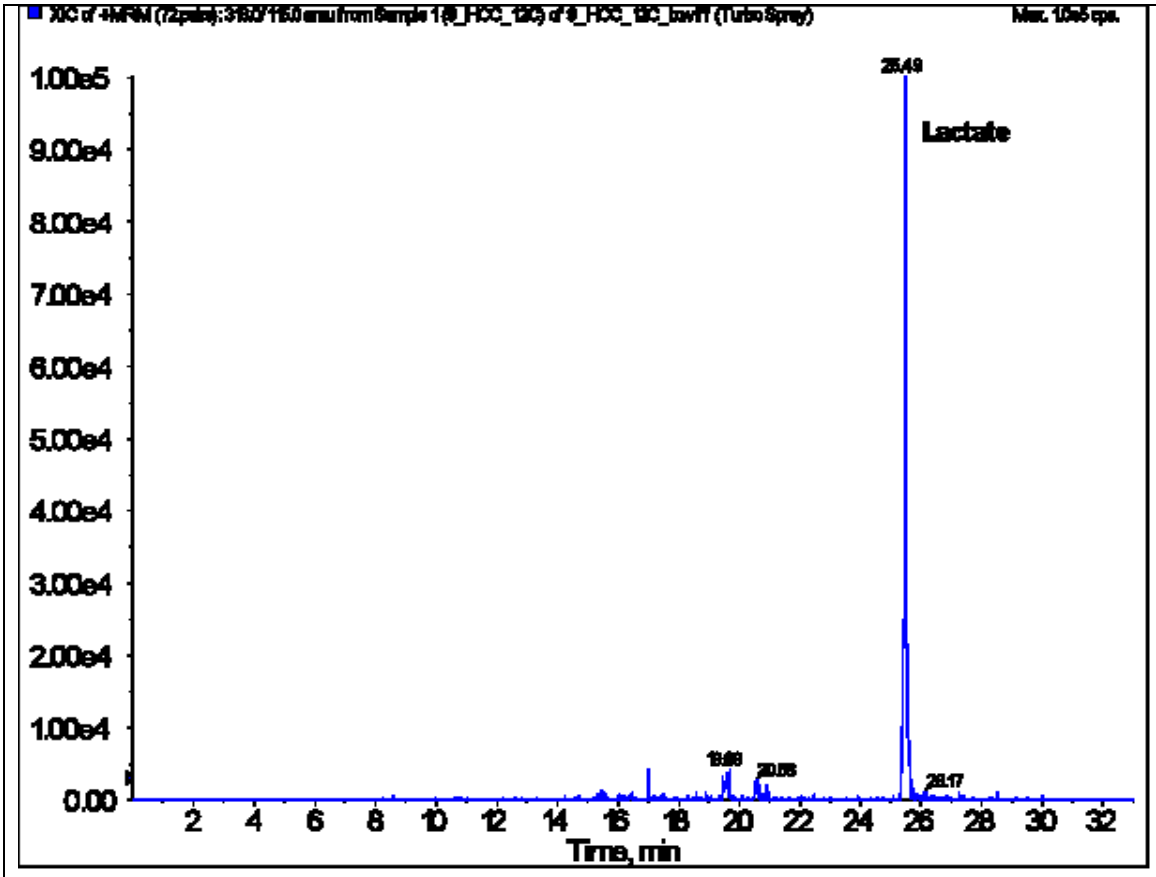

Figure 15S: LC-MS/MS Chromatograms of MTBSFA derivatived lactate of ^{13}C-labeled HCC cells. Plotted as signal intensity (cps, counts per second) versus retention time (min, minute).

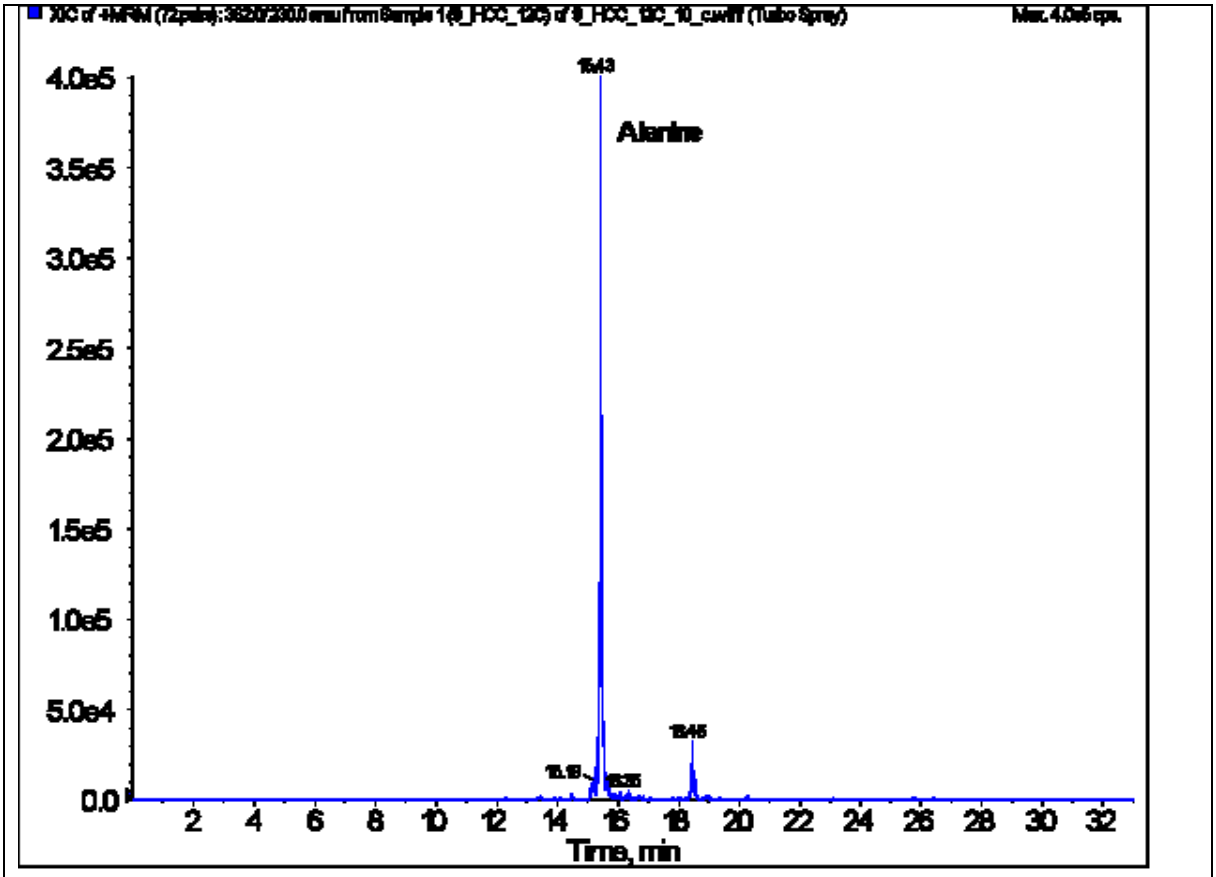

Figure 16S: LC-MS/MS Chromatograms of MTBSFA derivatived alanine of ^{13}C-labeled HCC cells. Plotted as signal intensity (cps, counts per second) versus retention time (min, minute).

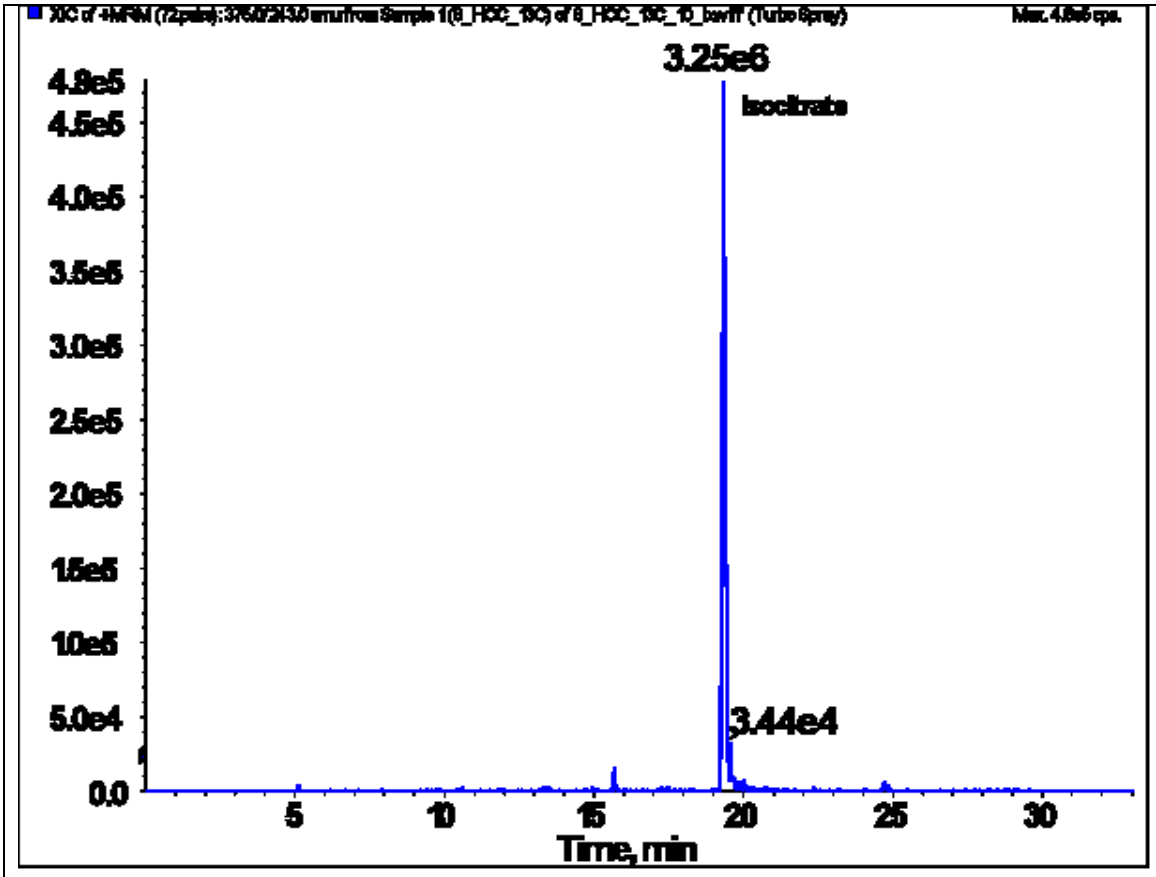

Figure 17S: LC-MS/MS Chromatograms of MTBSFA derivatived isocitrate of ^{13}C-labeled HCC cells. Plotted as signal intensity (cps, counts per second) versus retention time (min, minute).

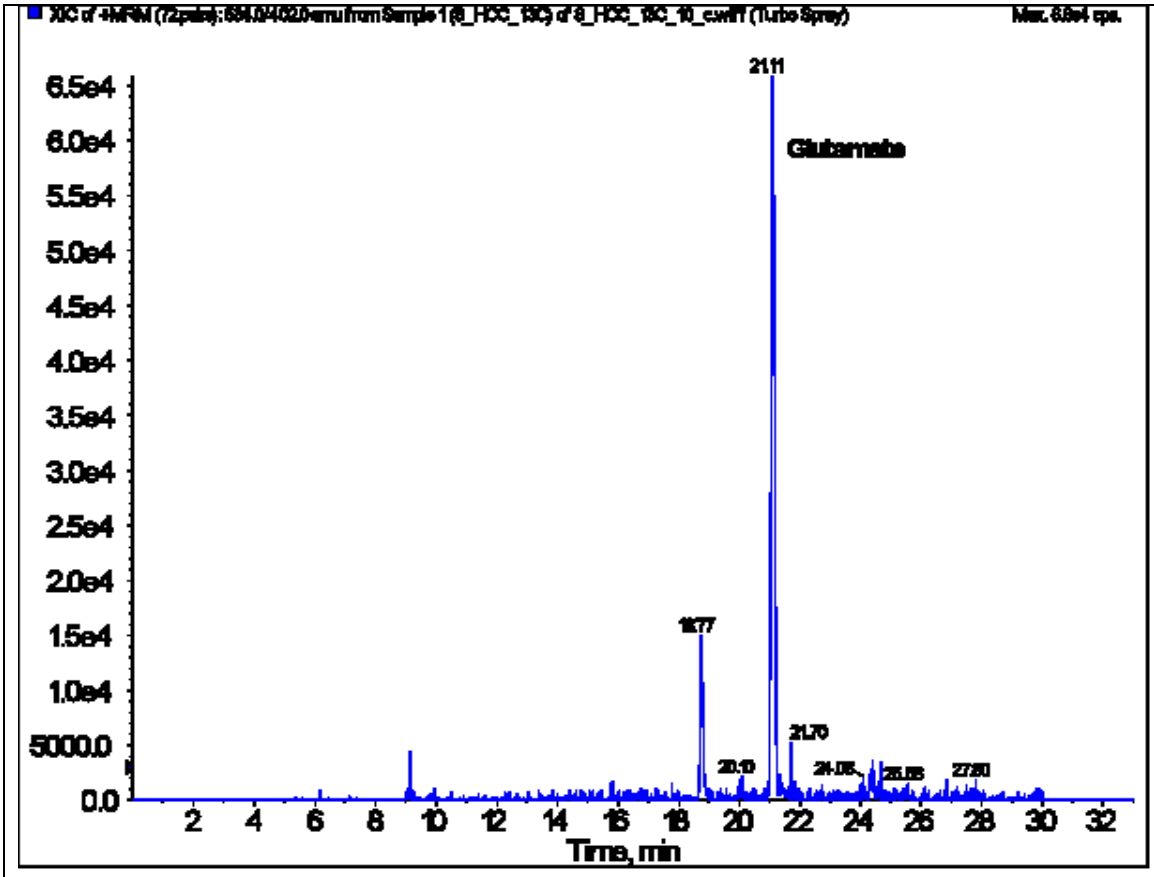

Figure 18S: LC-MS/MS Chromatograms of MTBSFA derivatived glutamate of ^{13}C-labeled HCC cells. Plotted as signal intensity (cps, counts per second) versus retention time (min, minute).

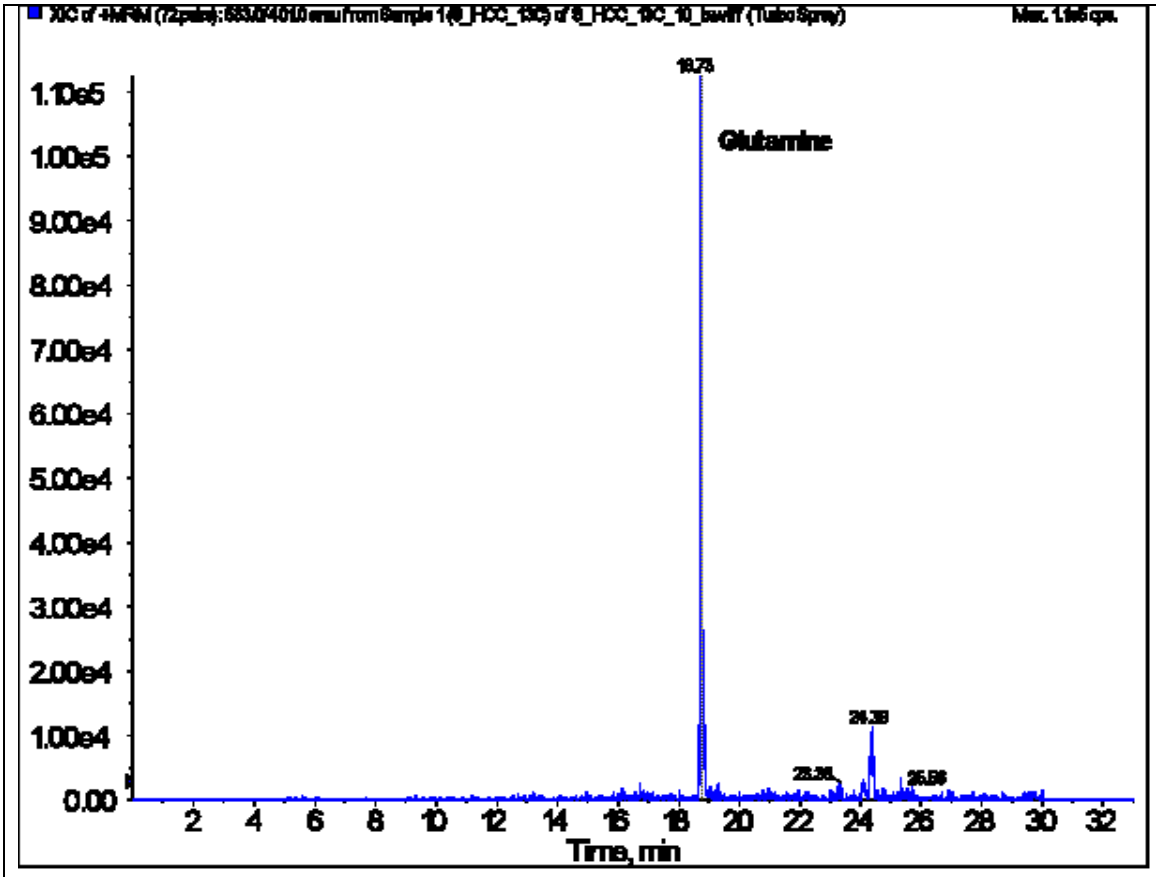

Figure 19S: LC-MS/MS Chromatograms of MTBSFA derivatived glutamine of ^{13}C-labeled HCC cells. Plotted as signal intensity (cps, counts per second) versus retention time (min, minute).

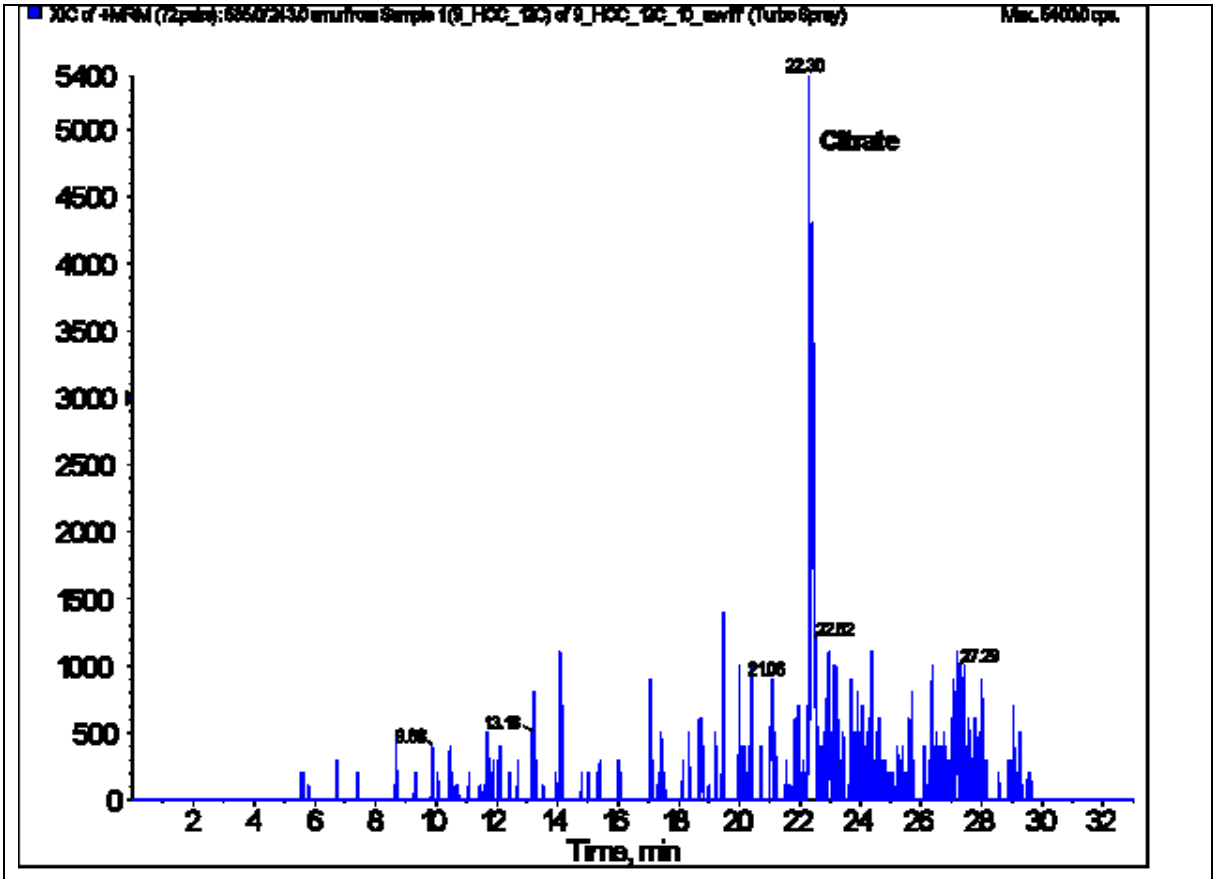

Figure 20S: LC-MS/MS Chromatograms of MTBSFA derivatived citrate of unlabeled HCC cells. Plotted as signal intensity (cps, counts per second) versus retention time (min, minute).

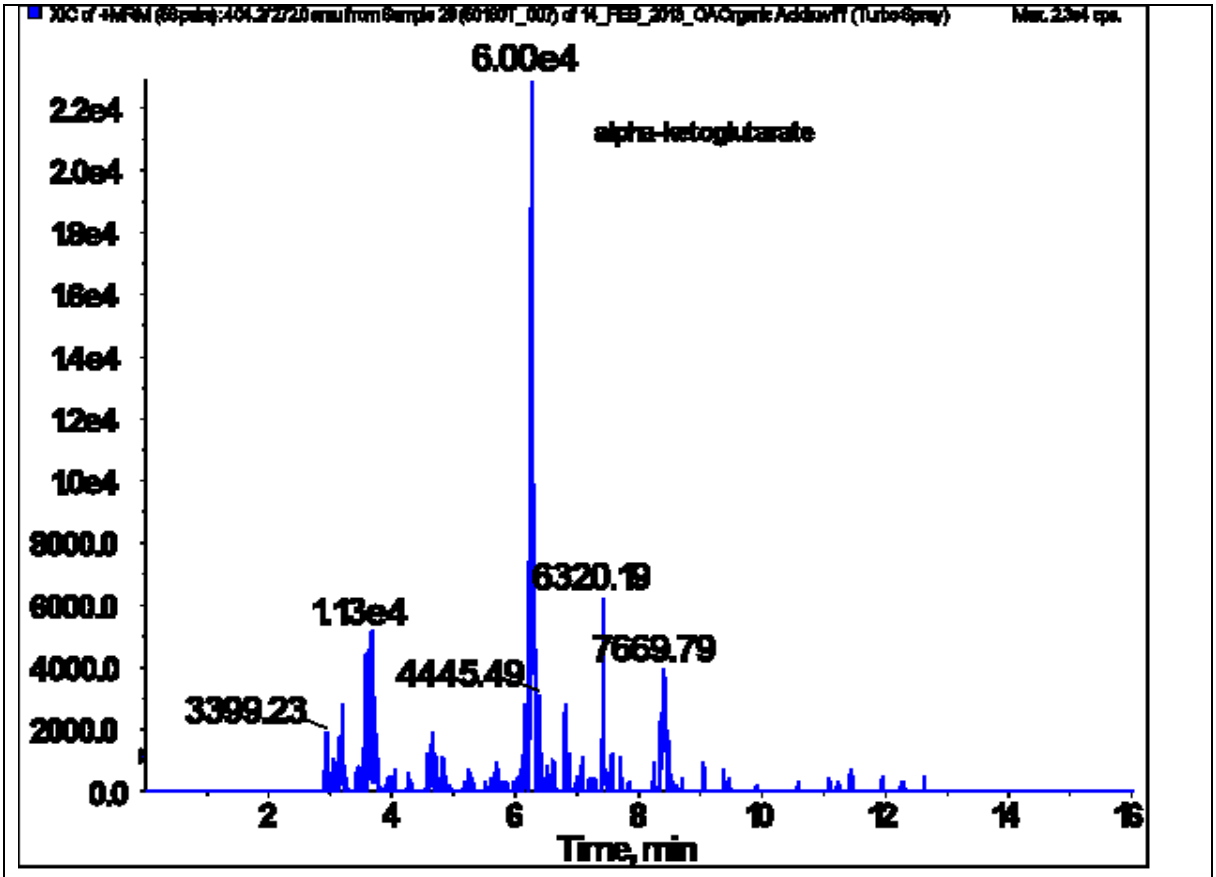

Figure 21S: LC-MS/MS Chromatograms of methoxylamine and MTBSFA derivatived α-ketoglutarate of unlabeled human HCC tissue. Plotted as signal intensity (cps, counts per second) versus retention time (min, minute).

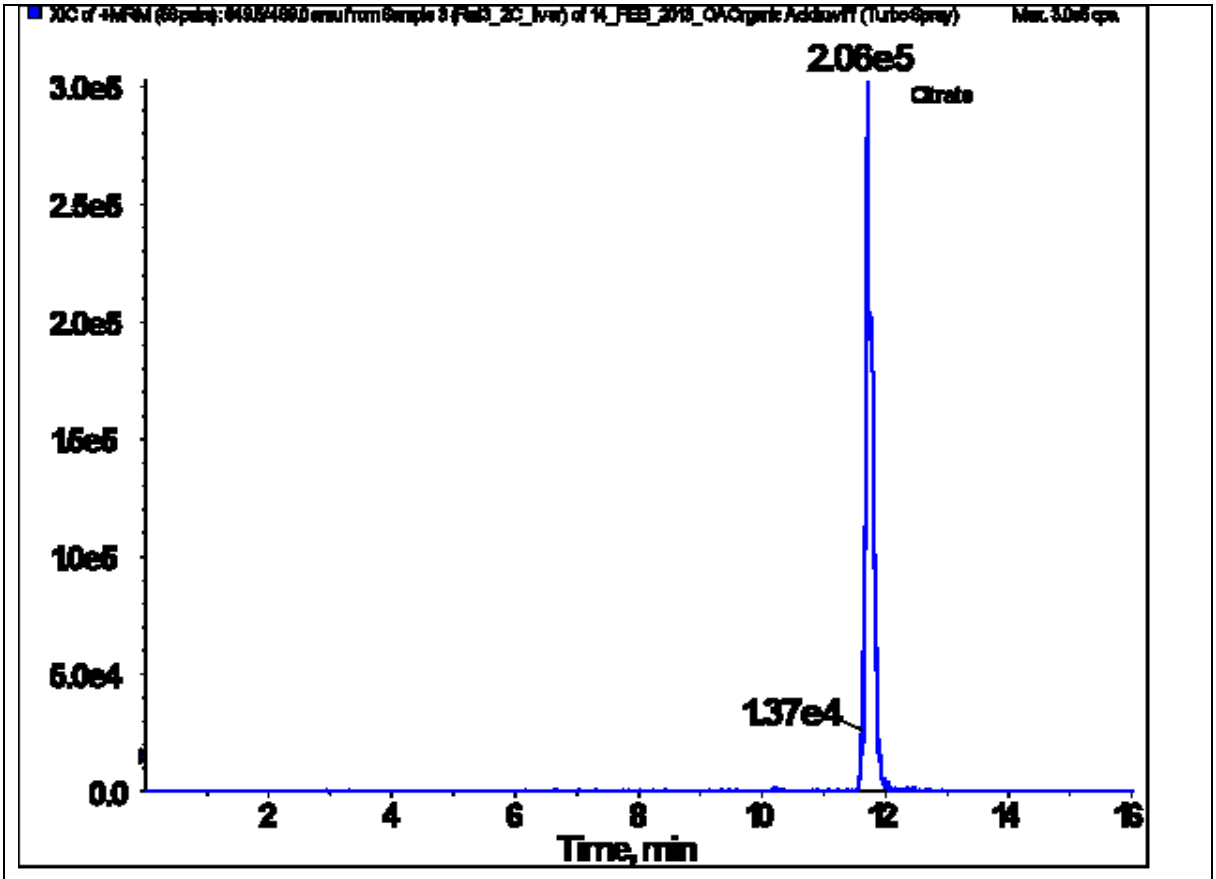

Figure 22S: LC-MS/MS Chromatograms of methoxylamine and MTBSFA derivatived citrate of unlabeled rat liver tissue. Plotted as signal intensity (cps, counts per second) versus retention time (min, minute).

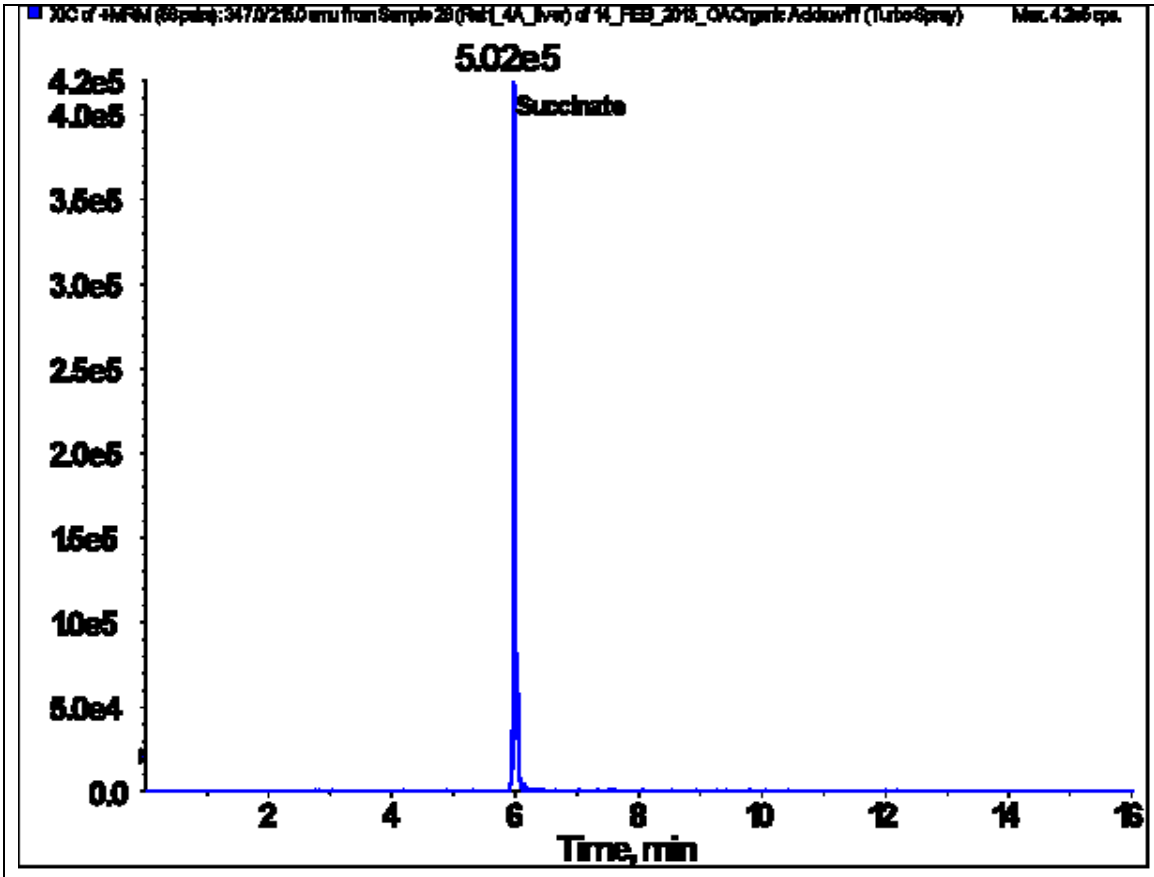

Figure 23S: LC-MS/MS Chromatograms of methoxylamine and MTBSFA derivatived succinate of unlabeled rat liver tissue. Plotted as signal intensity (cps, counts per second) versus retention time (min, minute).

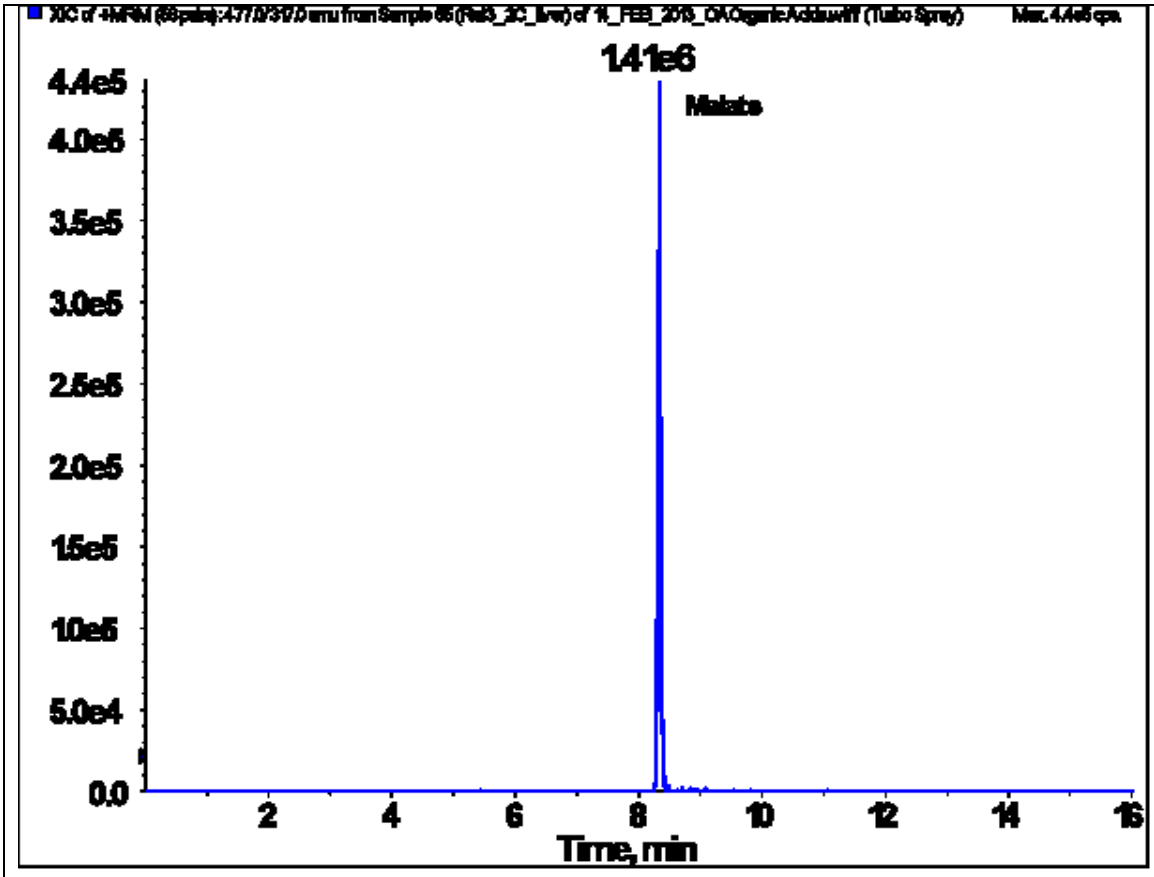

Figure 24S: LC-MS/MS Chromatograms of methoxylamine and MTBSFA derivatived malate of unlabeled rat liver tissue. Plotted as signal intensity (cps, counts per second) versus retention time (min, minute).

REFERENCES

1. Basu SS, Blair IA. Rotenone-mediated changes in intracellular coenzyme A thioester levels: Implications for mitochondrial dysfunction. *Chemical Research in Toxicology* 2011; **24**:1630-1632.
2. Bennett BD, Yuan J, Kimball EH, Rabinowitz JD. Absolute quantitation of intracellular metabolite concentrations by an isotope ratio-based approach. *Nature Protocols* 2008; **3**(8):1299-1311.
3. Fernandez CA, Rosiers CD, Previs SF, David F, Brunengraber H. Correction of 13C mass isotopomer distributions for natural stable isotope abundance. *Journal of Mass Spectrometry* 1996; **31**:255-262.
4. Tomcik K, Ibarra RA, Sadhukhan S, Han Y, Tochtrop GP, Zhang G-F. Isotopomer enrichment assay for very short chain fatty acids and its metabolic applications. *Analytical Biochemistry* 2011; **410**:110-117.